

Grasp a Moving Target from the Air: System & Control of an Aerial Manipulator *

Guangyu Zhang, Yuqing He, Bo Dai, Feng Gu, Liying Yang, Jianda Han, Guangjun Liu and Juntong Qi

Abstract— Grasping a moving target has been investigated extensively for fixed-base manipulator. However, such a task becomes much more challenging when the manipulator is free flying in the air with an UAV. Towards moving target grasping, this paper presents an aerial manipulator system composed of a hex-rotor and a 7-DoF (Degree of Freedom) manipulator. An independent control structure is used in the aerial manipulator control system, i.e., the hex-rotor and the manipulator are controlled separately. In the hex-rotor’s controller, the system CoM (Center of Mass) offset motion is used to compensate disturbance of the robotic arm. In the manipulator’s controller, the relative kinematics between the target and the aerial vehicle is taken into consideration to grasp the target. At last aerial grasping experiments are conducted to validate the feasibility of the proposed control scheme and the reliability of our aerial manipulator system.

I. INTRODUCTION

In recent years, aerial manipulation is becoming a new researching hotspot in the field of UAV [1], [2]. Usually, an aerial manipulator is composed of a rotorcraft UAV and a multi-link robotic arm. It combines the strong maneuverability of a UAV with the capability of a manipulator, leading to a broad application prospect. For example, a dual-arm aerial manipulator is designed in [3] to screw the valve. In [4], an aerial manipulator prototype for canopy sampling is presented. In [5]–[7], towards interaction tasks, aerial manipulator with compliant manipulator is designed.

Aerial grasping is a common task used to demonstrate the basic ability of the aerial manipulator. It will be very useful in many real applications, such as the sampling collection in special region, pick and place the dangerous objects in the terrorist sense, capture of moving target (e.g. small UAV). There has been some research on this topic. In [8], [9], a compliance and adaptive gripper is installed on a helicopter, which is able to grasp unstructured static objects in hovering flight mode. In [10], mimicking an agile that captures a moving prey, an aerial manipulator composed of a quadrotor and a 1-DoF arm is used to grasp a tubular object at high speeds. In [11], the aerial manipulator system composed of a

helicopter platform and a fully actuated 7-DoF redundant industrial robotic arm is able to grasp a pole and pull it out from a static hole. In [12], a pick-and-place task is completed by an aerial manipulator system using nonlinear model-predictive control methodology. In [13], using a high accuracy visual servoing algorithm, an aerial manipulator can grasp an object with 2cm precision.

It is not easy for an aerial manipulator to grasp a target, because the position control of a UAV needs to provide adequate accuracy to keep the target in the operational space of the manipulator, while the manipulator is moving and operating. As far as the authors know, published works on aerial grasping have focused on static objects, and the UAV is only required to be in hovering mode. If a moving object is considered, the level of difficulty will increase significantly. When the aerial manipulator is in a tracking mode, the coupling effect between the UAV and the manipulator becomes more severe. For this reason, the control accuracy of the UAV in the tracking mode will decrease, so the risk of missing the target from the operational space will increase.

Some investigation on aerial manipulator dynamic model and nonlinear control has been published in the literature, aiming to solve the system control problem theoretically. In [14], [15] the dynamic model of an aerial manipulator with 6+n DoF is derived through Euler-Lagrange equation, and a Cartesian impedance controller is designed to realize the hovering of an aerial manipulator in contact mode. In [16], the dynamic model of quadrotor with n DoF of manipulator is proposed, and a backstepping-like end-effector tracking control controller is designed based on the dynamic model. Such sophisticated control methods base on high dimension nonlinear dynamic mode are rarely used in real aerial manipulator system to complete practical tasks.

In this paper, aiming at the moving object grasping tasks, system design and control synthesis of an aerial manipulator system are presented. The main contribution of this paper lies in the following three aspects: 1) an aerial manipulator platform is developed particularly for moving object grasping experimentation; 2) a control strategy based on separate control of the UAV and the manipulator is proposed to make the whole grasping process safe and steady; and 3) aerial grasping experiments are conducted and the data are analyzed in detail. The results have shown the feasibility and validity of moving target grasping from the air with the proposed method.

The rest of this paper is organized as follows. In Section II the new aerial manipulator system and experimental platform are introduced. After that, the dynamical model of the aerial vehicle with the CoM offset and the relative kinematics are presented in Section III. Subsequently, control scheme and algorithm are given in Section IV, which is followed by the

* This work is supported by National Nature Sciences Foundation of China (Grant No.61433016 and No.U1608253).

Guangyu Zhang and Bo Dai are Ph.D. candidates at the State Key Laboratory of Robotics, Shenyang Institute of Automation, CAS, Shenyang 110016, China & University of Chinese Academy of Sciences, Beijing 100049, China (e-mail: zhangguangyu, daibo@sia.cn).

Yuqing He, Feng Gu, Liying Yang and Jianda Han are all with the State Key Laboratory of Robotics, Shenyang Institute of Automation, CAS, Shenyang 110016, China (e-mail: heyuqing, fenggu, yangliying, jdhan@sia.cn).

Guangjun Liu is with the Department of Aerospace Engineering, Ryerson University, Toronto, ON M5B 2K3 Canada (e-mail: gjliu@ryerson.ca).

Juntong Qi is with School of Electrical and Information Engineering, Tianjin University, Tianjin 300072, China (e-mail: qijt@tju.edu.cn)

experiments in Section V. Finally, conclusion, discussion and future work are presented in Section VI.

II. OVERVIEW OF AERIAL MANIPULATOR SYSTEM

A. Hardware of Aerial Manipulator

The proposed aerial manipulator system is shown in Fig. 1. It mainly consists of a hex-rotor UAV, a 7-DoF robotic arm and an under-actuated gripper. The main parameters of the aerial manipulator are listed out in Table I and Table II.

The tuned propulsion system of the hex-rotor is E800 of DJI powered by a 6 cells Li-po battery. The flight stack of the hex-rotor is an open source controller for autonomous drones named PixHawk [17]. The robotic arm is composed of Dynamixel smart actuators. The computer used as the arm controller is Intel NUC with a core-i7 processor. The under-actuated gripper is designed based on the Yale OpenHand Project by changing some structure and parameters [18]. The gripper is passively compliant and is capable of grasping objects adaptively [19].

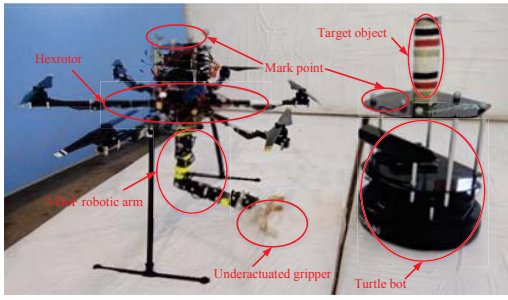


Figure 1. Composition of the aerial manipulator system

The moving target is a cylindrical object with 6cm diameter, 24cm height and 90g weight (as shown in Fig. 1). It is placed on a ground robot, ‘Turtle bot’, so that it can move on the ground freely.

The aerial grasping experiments are conducted in the OptiTrack, an indoor motion capture system. This system can provide position and orientation information of the marked object (the detailed information about the OptiTrack can be seen in[20]).

TABLE I. PARAMETERS OF THE HEX-ROTOR

Parameter	Value
Diagonal size	80 cm
Frame height	40 cm
Mass	3 kg
Max. takeoff weight	5.5 kg
Flight time	15 min

TABLE II. PARAMETERS OF THE MANIPULATOR

Parameter	Value
Arm Mass	1.5kg
Arm length l	53.4cm

Maximum open of gripper	12cm
-------------------------	------

B. Software Architecture of Aerial Manipulator

The software structure of the aerial manipulator is shown in Fig. 2. It mainly consists of three modules: state estimation module, hex-rotor control module and manipulator control module.

The state estimation module uses an EKF estimator to estimate the states of the hex-rotor and the target object in the inertial coordinate system based on the information of the OptiTrack and the IMU.

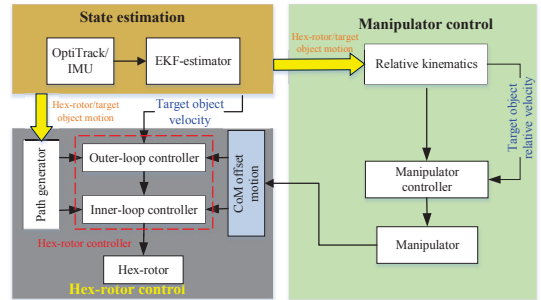


Figure 2. Software structure of aerial manipulator system

The hex-rotor control module is composed of the path generator and hex-rotor controller. The path generator generate the waypoint of hex-rotor to keep the target object in the operational space of the aerial manipulator. The hex-rotor controller is an inner-outer loop based PID controller that uses system CoM offset motion information to compensate the disturbance of the manipulator.

The manipulator control module is composed of relative kinematics module and manipulator controller. The relative kinematics module translates the target motion into the body frame. The manipulator controller is independent-joint based controller and uses the velocity feedforward to make the end effector track the moving target.

III. DYNAMIC MODEL

In this section, we will first construct the rigid body dynamics of aerial vehicle with a CoM offset, then the relative kinematics of the target relative to the aerial manipulator is introduced.

A. Dynamics of the Aerial Vehicle

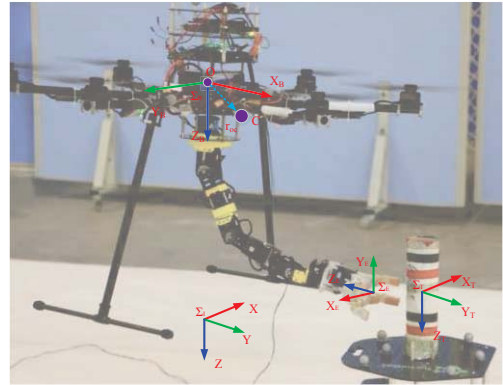


Figure 3. Coordinate frames of aerial manipulator system

The coordinate frames of the whole system are defined as shown in Fig. 3, where Σ_I , Σ_B , Σ_E , and Σ_T denote the NED inertial frame, the body fixed frame of the hex-rotor, the end-effector frame of the manipulator and the frame fixed on the target object, respectively. Point O is the coordinate origin of Σ_B and it coincides with the CoM of the hex-rotor.

The CoM of the whole aerial manipulator system is denoted by point C . Position of C is changing when the manipulator is moving, i.e., it is a function of the manipulator's joint angle. Here we use r_{OC} to denote the relative position between point O and point C , i.e., the CoM offset.

The position of aerial vehicle with respect to Σ_I is denoted by $p_b = [x, y, z]^T$, and its attitude is described by the Z-Y-X Euler angles $\Phi_b = [\varphi, \theta, \psi]^T$, denoting roll, pitch and yaw angle respectively. R_b denotes rotation matrix from Σ_B to Σ_I , and expressed as follows,

$$R_b = \begin{bmatrix} c\theta c\psi & s\phi s\theta c\psi - c\phi s\psi & c\phi s\theta c\psi + s\phi s\psi \\ c\theta s\psi & s\phi s\theta s\psi + c\phi c\psi & c\phi s\theta s\psi - s\phi c\psi \\ -s\theta & s\phi c\theta & c\phi c\theta \end{bmatrix} \quad (1)$$

where, c and s denote trigonometric function $\cos(\cdot)$ and $\sin(\cdot)$ respectively. We also define unit vectors e_1, e_2, e_3 , that is $I_{3 \times 3} = [e_1, e_2, e_3]$, where $I_{3 \times 3}$ is a unit matrix

We assume that the relative motion between the manipulator and the aerial vehicle is slow, which means that the velocity of the CoM offset is small. So that the dynamics of the aerial vehicle with CoM offset can be easily obtained through Newton-Euler equations, as in [21]. The final version is as follows,

$$\dot{p}_b = v_b \quad (2)$$

$$\dot{v}_b = g e_3 - \frac{1}{m} F R_b e_3 - R_b (\dot{\omega}_b^b \times r_{OC}^b(q) + \omega_b^b \times (\omega_b^b \times r_{OC}^b(q))) \quad (3)$$

$$\dot{R}_b = R_b \cdot S(\omega_b^b) \quad (4)$$

$$\dot{\omega}_b^b = I^{-1} (M - \omega_b^b \times (I \omega_b^b) + r_{OC}^b(q) \times F e_3) \quad (5)$$

where, v_b is velocity of the aerial vehicle with respect to Σ_I . g is the gravity acceleration. m is the mass of aerial manipulator system. F is total thrust generated by all rotating rotors. q is joint angle vector of the manipulator. $r_{OC}^b(q)$ is the CoM offset manipulator with respect to Σ_B , and it is a function of q . ω_b^b is the angle velocity of aerial vehicle with respect to Σ_B . $S(\cdot)$ is skew symmetric matrix function of a vector. I is inertia matrix of the aerial manipulator referenced to O . M is total moments acting on point O with respect to Σ_B . The terms with CoM offset, in Eq. (3) and Eq. (5), can partly describe the disturbance of the movement of the manipulator.

B. Relative Kinematics

The relative kinematics describes motion of the moving target relative to the aerial vehicle in the body fixed frame Σ_B . The absolute position and orientation of target object with respect to Σ_I are denoted by p_t and Φ_t respectively. p_{b-t}^b and Φ_{b-t}^b are position and orientation of the target object relative to aerial vehicle with respect to Σ_B . So we can get the relative displacement by following equations,

$$p_{b-t}^b = R_b^{-1}(p_t - p_b) \quad (6)$$

$$\Phi_{b-t}^b = R_b^{-1} \cdot \Phi_t \quad (7)$$

Then, relative velocity and angular velocity can be expressed as follows,

$$v_{b-t}^b = R_b^{-1}((v_t - v_b) + \omega_b^b \times (p_t - p_b)) \quad (8)$$

$$\omega_{b-t}^b = R_b^{-1}(\omega_t - R_b \omega_b^b) \quad (9)$$

where, v_{b-t}^b and ω_{b-t}^b are relative velocity and angular velocity respect to Σ_B . v_t and ω_t are absolute velocity and angular velocity of the target object.

IV. SYSTEM CONTROL

In this section, we introduce the path generator, hex-rotor controller with CoM offset compensation and the manipulator controller.

A. Path Generator

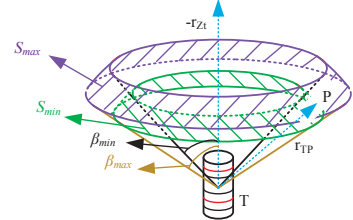


Figure 4. Safe operational space Ω of the target object

To generate appropriate position reference of the hex-rotor when the aerial manipulator grasping the moving target object, we firstly define a safe operational space Ω , in which the aerial manipulator is able to grasp the target object while the target object is kept away from the hex-rotor with a safe distance.

As shown in Fig. 4, the space Ω is a space around the target object. The space is part of the space between two concentric spherical surfaces (S_{min} and S_{max}), whose center is point T (the center of the target) and whose radius are l_{min} and l_{max} . The area is also limited in two conical surfaces which are coaxial with the cylindrical target object. The cone angle of the conical surface are β_{min} and β_{max} . So the point in the space Ω will satisfy the following inequalities.

$$l_{min} \leq \|r_{TP}\| \leq l_{max} \quad (10)$$

$$\beta_{min} \leq \langle -r_{Zt}, r_{TP} \rangle \leq \beta_{max} \quad (11)$$

where r_{TP} is the vector from point T to point P (any point in space Ω). r_{Zt} is the unit coordinate axis vector of Σ_T . $\langle -r_{Zt}, r_{TP} \rangle$ denotes the angle between $-r_{Zt}$ and r_{TP} . So the Eq. (10) and Eq. (11) limit the distance and orientation between the hex-rotor and the target object respectively. The values of l_{max} , l_{min} , β_{min} and β_{max} are determined by offline grasping tests.

To keep the aerial manipulator in the safe operational space Ω during grasping, the hex-rotor's position reference is set depending on its current position and target's position. We define that r_{Tp_b} is the vector from the target point to current position of hex-rotor and r_{Tp_b-d} is the vector from the target

point to desired position. r_k is the unit vector perpendicular to r_{Zt} and r_{Tpb} . If we rotate r_{Tpb} around r_k to the conical surfaces we can get vector r'_{Tpb} . The desired position of UAV can be determined by the following equations.

$$r'_k = \frac{-r_{Zt} \times r_{Tpb}}{\|r_{Tpb}\|} \quad (12)$$

$$r'_{Tpb} = \begin{cases} R_{r_k}(\beta_{min} - \langle -r_{Zt}, r_{Tpb} \rangle) r_{Tpb}, & \langle -r_{Zt}, r_{Tpb} \rangle \leq \beta_{min} \\ R_{r_k}(\beta_{max} - \langle -r_{Zt}, r_{Tpb} \rangle) r_{Tpb}, & \langle -r_{Zt}, r_{Tpb} \rangle \geq \beta_{max} \\ r_{Tpb}, & \text{others} \end{cases} \quad (13)$$

$$r'_{Tpb-d} = \begin{cases} l_{min} \cdot \frac{r'_{Tpb}}{\|r'_{Tpb}\|}, & \|r'_{Tpb}\| \leq l_{min} \\ l_{max} \cdot \frac{r'_{Tpb}}{\|r'_{Tpb}\|}, & \|r'_{Tpb}\| \geq l_{max} \\ r'_{Tpb}, & \text{others} \end{cases} \quad (14)$$

$$p_{b,d} = p_t + r'_{Tpb-d} \quad (15)$$

where, $R_{r_k}(\alpha)$ is the rotation matrix representing a

track desired attitude, $\Phi_{b,d} = [\varphi_d, \theta_d, \psi_d]^T$. ΔF and ΔM are the manipulator disturbance compensation terms (terms of system CoM offset), which will be detailed in the remainder of this section.

First, for the position P controller, it can be denoted as the following equation:

$$v_{b,d} = K_{p,pb} e_{pb} + v_t \quad (16)$$

where, $v_{b,d}$ is the desired velocity. $e_{pb} = p_{b,d} - p_b$, $K_{p,pb}$ is the proportional gain matrix of the position P controller. v_t is the target object velocity used as a feed-forward term.

Then, the velocity PID controller that use velocity error, $e_{vb} = v_{b,d} - v_b$, to generate desired thrust, F_d , and desired attitude angle, roll, φ_d , pitch, θ_d , is expressed as follow,

$$F_d = \left\| K_{p,vb} e_{vb} + K_{i,vb} \int e_{vb} dt + K_{d,vb} \frac{de_{vb}}{dt} - \Delta F \right\| \quad (17)$$

$$\Delta F = \omega_b^b \times (\omega_b^b \times r_{OC}^b(q)) \quad (18)$$

where, $K_{p,vb}$, $K_{i,vb}$ and $K_{d,vb}$ are gain matrices of the velocity PID controller. ΔF is the term is used to compensate the disturbance of manipulator in the translational dynamic of hex-rotor, as Eq. (3).

Since φ and θ can be obtained through rotational matrix R_b as in Eq. (1). φ_d and θ_d can also be replaced by the desired

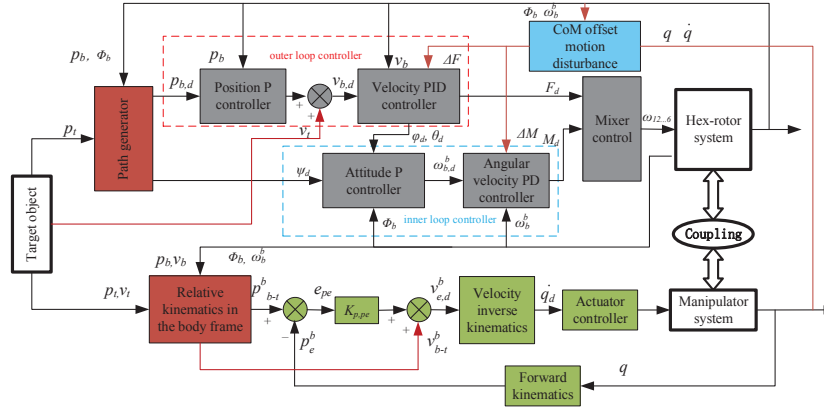


Figure 5. The system control structure

rotation transformation that rotating around r_k with α radians. From Eq. (12)-Eq. (15), we can know that when the hex-rotor is in the space Ω the desired position is set to be the current position, $p_{b,d} = p_b$, otherwise the desired position is set to be the nearest point in the space Ω to the hex-rotor. The yaw desired angle is always set to point to the target

B. Aerial Vehicle Control

The hex-rotor controller is based on the inner-outer loop control structure, as shown in Fig. 5. The position P controller and velocity PID controller compose the outer loop controller that generates the reference roll, φ_d , pitch, θ_d , and desired thrust, F_d , to track the desired position, $p_{b,d}$. The attitude P controller and angular velocity PD controller compose the inner loop controller that generates desired moment, M_d , to

rotation matrix, $R_{b,d} = [b_{x,d}, b_{y,d}, b_{z,d}]$. As in [22], we can obtain it using the following equations:

$$b_z = \frac{K_{p,vb} e_{vb} + K_{i,vb} \int e_{vb} dt + K_{d,vb} \frac{de_{vb}}{dt} - \Delta F}{\left\| K_{p,vb} e_{vb} + K_{i,vb} \int e_{vb} dt + K_{d,vb} \frac{de_{vb}}{dt} - \Delta F \right\|} \quad (19)$$

$$b_y = b_z \times [c\psi_d \quad s\psi_d \quad 0]^T \quad (20)$$

$$b_x = b_y \times b_z \quad (21)$$

Based on the preceding desired rotation matrix, the attitude controller is then used to get the desired angular velocity, $\omega_{b,d}^b$. The details are as follows

$$e_{Rb} = \frac{1}{2} S^{-1} (R_{b,d}^{-1} R_b - R_b^{-1} R_{b,d}) \quad (22)$$

$$\omega_{b,d}^b = K_{p,Rb} e_{Rb} \quad (23)$$

where, e_{Rb} is the attitude error. $S^{-1}(\cdot)$ is the inverse function of $S(\cdot)$. $K_{p,Rb}$ is the proportional gain matrix of the attitude P controller.

Finally, the angular velocity controller is as following equation,

$$M_d = K_{p,\omega b} e_{\omega b} + K_{d,\omega b} \frac{de_{\omega b}}{dt} - \Delta M \quad (24)$$

$$\Delta M = r_{oc}^b(q) \times F_d e_3 \quad (25)$$

where $K_{p,\omega b}$, and $K_{d,\omega b}$ are gain matrices of the angular velocity PD controller. $e_{\omega b} = \omega_{b,d}^d - \omega_b^b$ is the angular velocity error.

The term ΔM is used to compensate the disturbance of the manipulator in the rotational dynamic of the hex-rotor, as in Eq. (5).

C. Manipulator control

The manipulator controller structure is shown in Fig. 5. The manipulator is controlled in the body fixed frame, Σ_B . To grasp the target, we first use the relative kinematics to get the relative position, $p_{b,e}^b$ (Eq. (6)), and use it as the desired position of the manipulator end-effector. The position is controlled by a P controller with a velocity feed-forward, $v_{b,t}^b$, to get desired velocity of the manipulator end-effector, $v_{e,d}^b$. Then through the velocity inverse kinematics we can get the desired joint rates, \dot{q}_d , of the actuators which have low level controller to track joint rates reference with enough accuracy.

The theme of velocity inverse kinematics is to find the right joint rate that can generate desired velocity of the manipulator end-effector. We use v_e^b and ω_e^b to denote linear velocity and angular velocity of end-effector with respect to Σ_B respectively. So the manipulator Jacobian equation is

$$V = \begin{bmatrix} v_e^b \\ \omega_e^b \end{bmatrix} = J_e^b(q) \dot{q} \quad (26)$$

where, $J_e^b(q)$ (6×7) is the manipulator Jacobian. The velocity inverse kinematics is also called velocity control of manipulator. The velocity control of redundant manipulator have a framework that is introduced in [23], and it can be described as follow equation,

$$\dot{q}_d = \left[\frac{J_e^b(q)}{N_J^T W} \right]^{-1} \left[\begin{bmatrix} V_d \\ -\alpha N_J^T \Delta f \end{bmatrix} \right] \quad (27)$$

where, W is a symmetric positive-definite weighting matrix defining a joint rate measure through $\dot{q}^T W \dot{q}$. N_J is a matrix whose columns are a spanning set of the null space of $J_e^b(q)$, that is $J_e^b(q) N_J = 0$. α is a scalar, and Δf is the gradient of

$f(q)$ that is a function of the joint values. The \dot{q}_d given by Eq. (27) can satisfy Eq. (26) while minimizing $\frac{1}{2} \dot{q}^T W \dot{q} + \alpha \dot{f}(q)$.

A manipulator experiences a kinematic singularity whenever the manipulator Jacobian loses rank. To avoid singularities, $f(q)$ needs to be large at singularities and small away from singularities. For this, the damped inverse of the product of the singular values of a weighted Jacobian is used. That is, the optimization function is defined as in the following

$$f(q) = \frac{1}{\bar{\sigma}_1 \bar{\sigma}_2 \dots \bar{\sigma}_6 + \varepsilon} \quad (28)$$

where ε is a damping factor, and $\bar{\sigma}_i$ is singular value of the weighted Jacobian: $J_W = D_T J_e^b(q) D_J$. Where, D_T and D_J are diagonal matrices.

V. EXPERIMENTS AND RESULTS

We conduct experiments to validate the feasibility and the reliability of our aerial manipulator system. The first is the one that validates disturbance compensation performance of the hex-rotor controller while the robotic arm is moving freely. The second one is to use the aerial manipulator to grasp up a moving target to test its performance.

A. Manipulator Disturbance Compensation

To validate the disturbance compensation performance of terms of ΔF and ΔM presented in the section IV, we make the manipulator swing periodically when the aerial vehicle hovering without or with the compensation terms respectively. To make the manipulator swing periodically, we make the shoulder roll joint keeping in $\pi/4$, and make the shoulder pitch joint moving from $-\pi/2$ to $\pi/2$ periodically, as shown in Fig. 6.

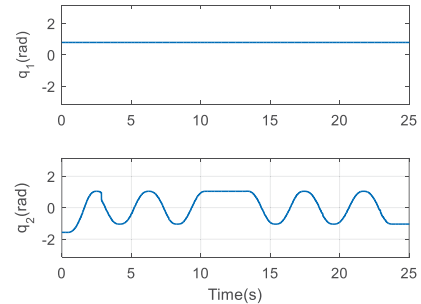


Figure 6. The first and the second joint trajectory of the manipulator

The position error and the attitude error in this experiment are shown in Fig. 7. The mean and variance of absolute value of errors are shown in Table III. In the first period, from t=1s to t=12s, the hex-rotor is controlled by the controller without compensation terms. In the second period, from t=12s to t=25s the hex-rotor is controlled by the controller with compensation terms. From Fig. 7 and Table III, we can see that the amplitudes of the position and attitude error are smaller in the second period, and the mean of the error is decreased by half approximately. Contrasting the experiment results in the first and second period we can get that the compensation terms can partly compensate the disturbance of the manipulator and improve the control accuracy of the aerial vehicle significantly, which is necessary to keep the aerial vehicle in the safe

operational space Ω , while the manipulator is moving to grasp the target.

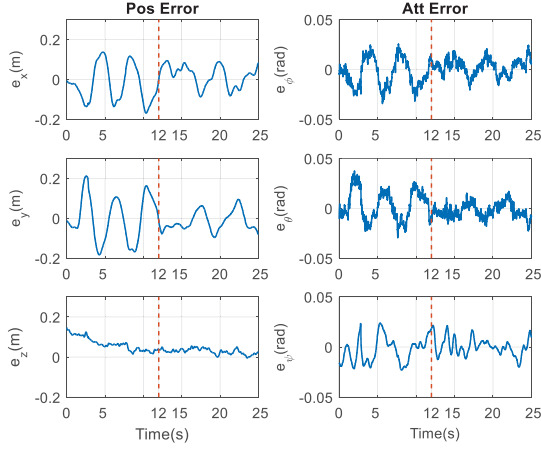


Figure 7. The position and attitude error of hex-rotor (in $t=1\text{-}12\text{s}$ and $t=12\text{-}25\text{s}$ the controller is without and with compensation terms respectively).

Contrasting the position and attitude error in every state, we can get that the control performance of x , y , ϕ and θ is worse than that of z and ψ , when the manipulator is moving.

Remark 1. The free moving manipulator causes degradation in performance of position and attitude control mainly in X and Y directions.

TABLE III. MEAN AND VARIANCE OF THE POSITION AND ATTITUDE ABSOLUTE VALUE OF ERROR

Parameter	$t=1\text{-}12\text{s}$		$t=12\text{-}25\text{s}$		
	mean	variance (10^{-3})	mean	variance (10^{-3})	
Position error	x	0.0431	0.4002	0.0233	0.1686
	y	0.0478	0.7500	0.0231	0.1550
	z	0.0272	0.1781	0.0137	0.0520
Attitude error	ϕ	0.0123	0.0550	0.0070	0.0223
	θ	0.0126	0.0638	0.0062	0.0180
	ψ	0.0109	0.0531	0.0055	0.0238

B. Aerial Grasping the Moving target

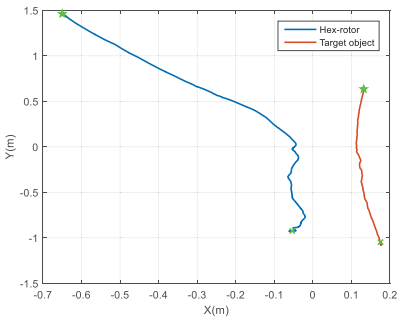


Figure 8. The trajectory of hex-rotor and target in the moving target grasping experiment (green pentagram is the start point, green cross is the end point).

The trajectory of hex-rotor and target in the moving target grasping experiment is shown in Fig. 8. The aerial manipulator flies toward to the target from start point and tracks it until grasping it up. The aerial grasping procedure is shown in Fig. 9.

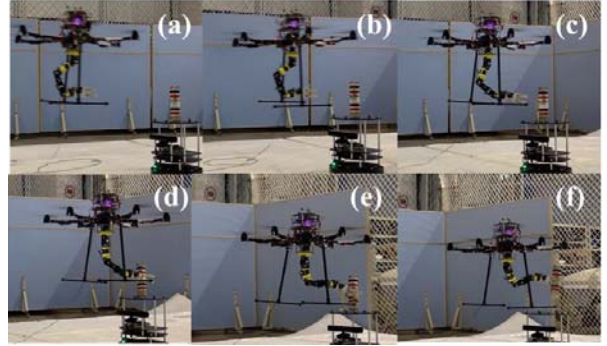


Figure 9. Aerial manipulator grasp a moving target

Step I: Before $t=7\text{s}$, the aerial manipulator flies toward to the target object and keep tracking it, as picture (a)-(b). In this period, the manipulator keep static.

Step II: From $t=7\text{s}$ to $t=10\text{s}$, the aerial manipulator keep in the safe operational space and the manipulator starts to approach the target, as picture (c). As shown in Fig. 10 and Fig. 11, when the manipulator starts to move, the position between end-effector and the target decreases, but the position control error of the hex-rotor increases because of the manipulator's disturbance,. If the hex-rotor controller without the compensation terms, the aerial manipulator will fly out the safe operational space, which will make it difficult to complete the grasping task. That is the better disturbance rejection performance of the aerial vehicle the higher probability of successful aerial grasping.

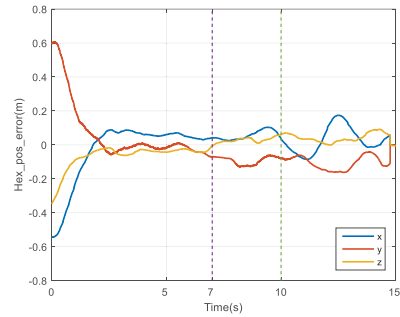


Figure 10. Position error of aerial vehicle when the aerial manipulator grasp a moving target

Step III: After $t=10\text{s}$, the manipulator tries to pull out the target object, as picture (d)-(e). In this period, the aerial vehicle's position control error become larger, especially X position error, as shown in Fig. 10. Because, when aerial manipulator keep contact manipulation, the disturbance mainly introduced by the environment, and it is large and uncertain. Under this condition, as in Fig. 11, the inverse relative kinematics of the manipulator control can keep the position between end-effector and the target object in the graspable space.

Remark 2. The disturbance of the manipulator in contact manipulation mode is larger than that in the free movement mode.

Step IV: The aerial manipulator finally grasps the moving target object.

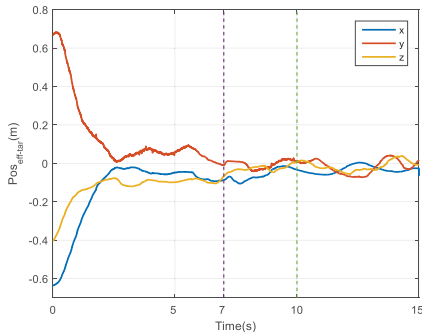


Figure 11. Position error between manipulator end-effector and the target object

VI. CONCLUSION

In this paper, we present an aerial manipulator system that can be used to grasp a moving target. It is composed of a hex-rotor and a 7-DoF manipulator and a control system with an independent control structure. The proposed hex-rotor controller can compensate for the disturbance due to the moving robotic arm by taking the system CoM offset into consideration.

In future work, our main attention will be on two aspects. First, aerial manipulator is a redundant robot system, and an optimal cooperative motion planning of the aerial vehicle and manipulator can weaken coupling effect significantly. Second, we will pay more attention to decrease the disturbance in contact manipulation using the impedance control approach.

REFERENCES

- [1] B. Yang, Y. He, J. Han, G. Liu, Z. Wang, and G. Zhang, "Survey on aerial manipulator systems," *Robot*, vol. 37, no. 5, pp. 627–640, 2015.
- [2] D. Song, X. Meng, Q. I. Junlong, and J. Han, "Strategy of Dynamic Modeling and Predictive Control on 3-Do F Rotorcraft Aerial Manipulator System," *Robot*, vol. 37, no. 2, pp. 152–160, 2015.
- [3] C. Korpela, M. Orsag, and P. Oh, "Towards valve turning using a dual-arm aerial manipulator," in *2014 IEEE/RSJ International Conference on Intelligent Robots and Systems*, 2014, pp. 3411–3416.
- [4] J. R. Kutia, K. A. Stol, and W. Xu, "Initial flight experiments of a canopy sampling aerial manipulator," in *2016 International Conference on Unmanned Aircraft Systems (ICUAS)*, 2016, pp. 1359–1365.
- [5] M. Fumagalli, S. Stramigioli, and R. Carloni, "Mechatronic design of a robotic manipulator for Unmanned Aerial Vehicles," in *2016 IEEE/RSJ International Conference on Intelligent Robots and Systems (IROS)*, 2016, pp. 4843–4848.
- [6] T. Bartelds, A. Capra, S. Hamaza, S. Stramigioli, and M. Fumagalli, "Compliant Aerial Manipulators: Toward a New Generation of Aerial Robotic Workers," *IEEE Robot. Autom. Lett.*, vol. 1, no. 1, pp. 477–483, Jan. 2016.
- [7] M. Kamel, K. Alexis, and R. Siegwart, "Design and modeling of dexterous aerial manipulator," in *2016 IEEE/RSJ International Conference on Intelligent Robots and Systems (IROS)*, 2016, pp. 4870–4876.
- [8] P. E. I. Pounds, D. R. Bersak, and A. M. Dollar, "The Yale Aerial Manipulator: Grasping in flight," in *2011 IEEE International Conference on Robotics and Automation*, 2011, pp. 2974–2975.
- [9] P. E. Pounds and A. M. Dollar, "Aerial Grasping from a Helicopter UAV Platform," in *Experimental Robotics*, Springer, Berlin, Heidelberg, 2014, pp. 269–283.
- [10] J. Thomas, G. Loianno, J. Polin, K. Sreenath, and V. Kumar, "Toward autonomous avian-inspired grasping for micro aerial vehicles," *Bioinspir. Biomim.*, vol. 9, no. 2, p. 025010, 2014.
- [11] F. Huber *et al.*, "First analysis and experiments in aerial manipulation using fully actuated redundant robot arm," in *2013 IEEE/RSJ International Conference on Intelligent Robots and Systems*, 2013, pp. 3452–3457.
- [12] G. Garimella and M. Kobilarov, "Towards model-predictive control for aerial pick-and-place," in *2015 IEEE International Conference on Robotics and Automation (ICRA)*, 2015, pp. 4692–4697.
- [13] M. Laiacker, F. Huber, and K. Kondak, "High accuracy visual servoing for aerial manipulation using a 7 degrees of freedom industrial manipulator," in *2016 IEEE/RSJ International Conference on Intelligent Robots and Systems (IROS)*, 2016, pp. 1631–1636.
- [14] V. Lippiello and F. Ruggiero, "Cartesian Impedance Control of a UAV with a Robotic Arm," *IFAC Proc. Vol.*, vol. 45, no. 22, pp. 704–709, Jan. 2012.
- [15] V. Lippiello and F. Ruggiero, "Exploiting redundancy in Cartesian impedance control of UAVs equipped with a robotic arm," in *2012 IEEE/RSJ International Conference on Intelligent Robots and Systems*, 2012, pp. 3768–3773.
- [16] H. Yang and D. Lee, "Dynamics and control of quadrotor with robotic manipulator," in *2014 IEEE International Conference on Robotics and Automation (ICRA)*, 2014, pp. 5544–5549.
- [17] L. Meier, D. Honegger, and M. Pollefeys, "PX4: A node-based multithreaded open source robotics framework for deeply embedded platforms," in *2015 IEEE International Conference on Robotics and Automation (ICRA)*, 2015, pp. 6235–6240.
- [18] "Yale OpenHand Project." [Online]. Available: <https://www.eng.yale.edu/grablab/openhand/>. [Accessed: 12-Sep-2017].
- [19] A. M. Dollar and R. D. Howe, "The Highly Adaptive SDM Hand: Design and Performance Evaluation," *Int. J. Robot. Res.*, vol. 29, no. 5, pp. 585–597, Apr. 2010.
- [20] "OptiTrack Documentation Wiki - NaturalPoint Product Documentation Ver 2.0." [Online]. Available: http://v20.wiki.optitrack.com//index.php?title=Main_Page. [Accessed: 12-Sep-2017].
- [21] I. Palunko, P. Cruz, and R. Fierro, "Agile Load Transportation : Safe and Efficient Load Manipulation with Aerial Robots," *IEEE Robot. Autom. Mag.*, vol. 19, no. 3, pp. 69–79, Sep. 2012.
- [22] T. Lee, M. Leoky, and N. H. McClamroch, "Geometric tracking control of a quadrotor UAV on $SE(3)$," in *49th IEEE Conference on Decision and Control (CDC)*, 2010, pp. 5420–5425.
- [23] J. D. English and A. A. Maciejewski, "On the implementation of velocity control for kinematically redundant manipulators," *IEEE Trans. Syst. Man Cybern. - Part Syst. Hum.*, vol. 30, no. 3, pp. 233–237, May 2000.